RESEARCH ARTICLE

Figures and figure supplements

The cAMP effector PKA mediates Moody GPCR signaling in *Drosophila* blood–brain barrier formation and maturation

Xiaoling Li *et al*

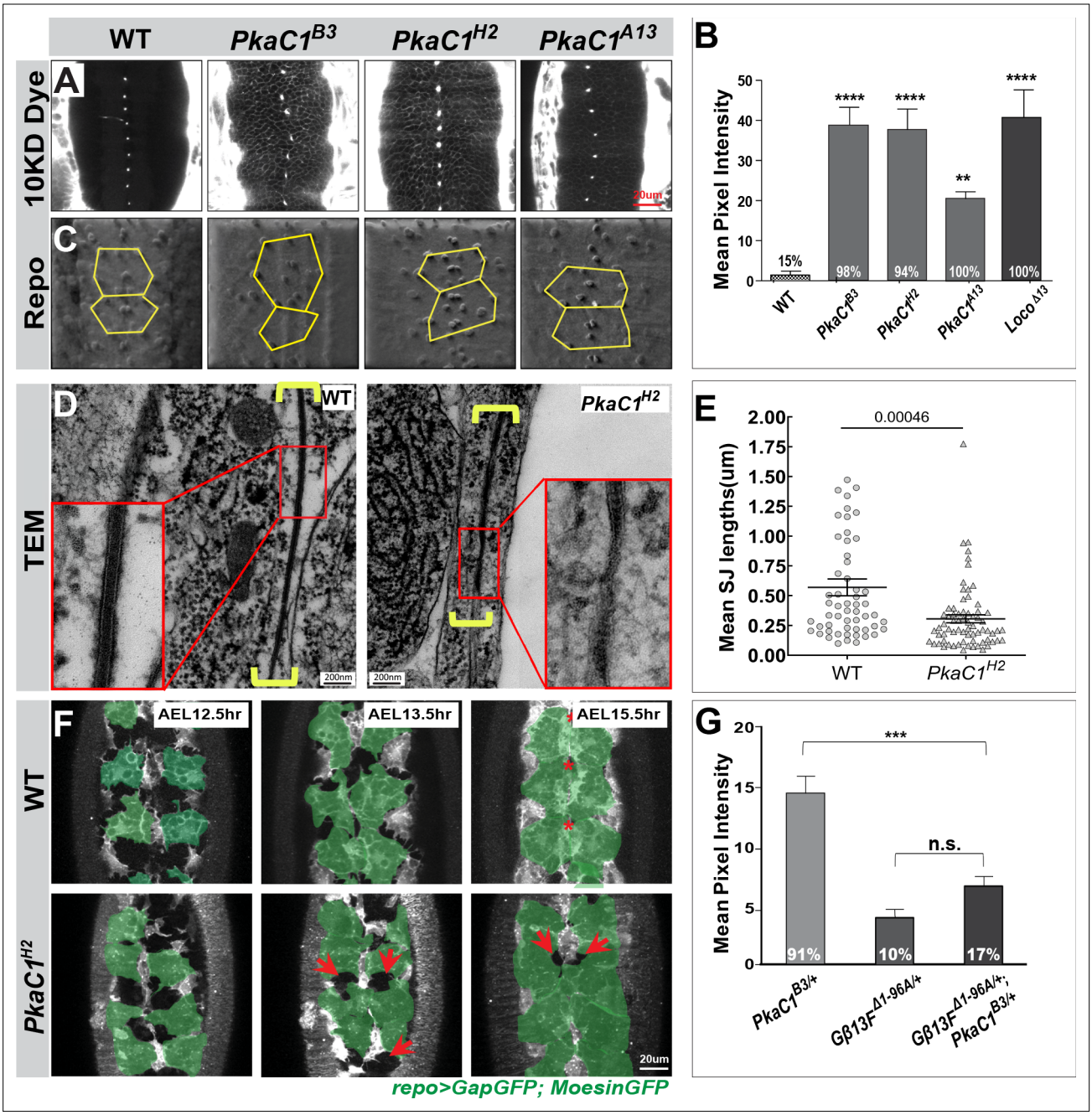

Figure 1. Protein kinase A (PKA) is required for blood–brain barrier (BBB) formation and acts in the Moody signaling pathway. (**A**) Single confocal sections of dye-injected embryos of WT and PKA zygotic mutants. (**B**) Quantification of the dye penetration assay. Columns represent the intensity of dye penetration into the nerve cord as measured by the mean pixel intensity (see Experimental procedures), ± SEM, n = 32, 31, 41, 38, 16 in WT, *PkaC1*^{B3}, *PkaC1*^{H2}, *PkaC1*^{A13}, *Loco*$^{\Delta 13}$ embryos, respectively. *Loco*$^{\Delta 13}$ zygotic mutants serve as positive controls. (**C**) Repo staining revealing the number and positions of subperineural glia (SPG) nuclei in WT and PKA zygotic mutants using an illuminated projection to highlight the ventral surface of the nerve cord. (**D**) Transmission electron micrographs of the interface of neighboring SPG in late WT and *PkaC1*^{H2} zygotic mutant embryos. Yellow brackets delineate the septate junction (SJ) ultrastructure; high magnifications are shown in red boxes. (**E**) Quantification of SJ length in WT and *PkaC1*^{H2} mutants (see Experimental procedures). Columns represent mean SJ length as measured in random nerve cord sections, ± SEM, n = 56 and n = 70 in WT and *PkaC1*^{H2} mutants, respectively. (**F**) Time-lapse recording of BBB closure in embryos of WT and *PKA* zygotic mutants. 6 µm confocal stacks are shown; in each image, 4–6 ventral SPG are highlighted (green); midline channels (stars) and retarded growth (arrows) are marked. (**G**) Dominant genetic interactions between *PkaC1*^{B3} and *Gβ13F*$^{\Delta 1\text{-}96A}$ as quantified by dye penetration in the embryo. Columns represent the intensity of dye penetration as measured by the mean pixel intensity, ± SEM, n = 34, n = 48, and n = 71 in *PkaC1*$^{B3/+}$, *Gβ13F*$^{\Delta 1\text{-}96A/+}$, and *Gβ13F*$^{\Delta 1\text{-}96A/+}$;*PkaC1*$^{B3/+}$ mutants, respectively. In (**B**) and (**G**), the percentage of embryos showing the dye penetration is indicated at the bottom of each column. Brackets and asterisks in (**B**), (**E**), and (**G**) indicate statistical significance levels as assessed by ordinary one-way ANOVA with Dunnett's multiple comparisons test in (**B**) and (**G**) or the two-tailed Student's t-test in (**E**), n.s., p>0.05; *p<0.05; **p<0.01; ***p<0.001.

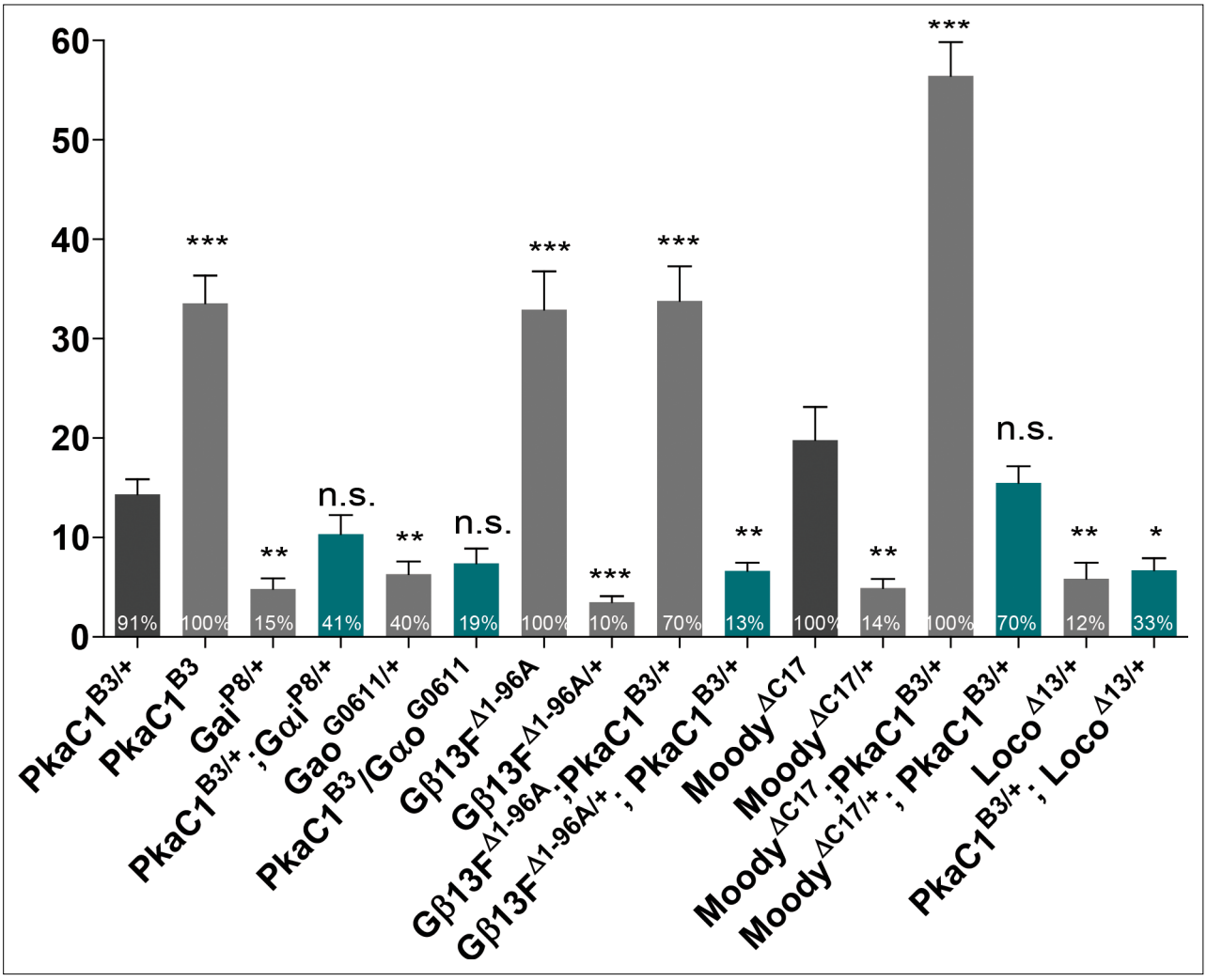

Figure 1—figure supplement 1. Genetic interactions between protein kinase A and different Moody pathway components. Quantitative analysis of dye penetration shows that the mild blood–brain barrier defect of *PkaC1*^{B3} heterozygotes can be partially rescued by removing one copy of G β 13F as well as one copy of Loco. The removal of one copy of other Moody pathway components, such as moody, Gαo, and Gαi, results in no or weaker, non-significant rescue, suggesting that G β 13F is more dosage sensitive. Asterisks indicate statistical significance levels as assessed by one-way ANOVA with Dunnett's multiple comparisons test, n.s., p>0.05; *p<0.05; **p<0.01; ***p<0.001.

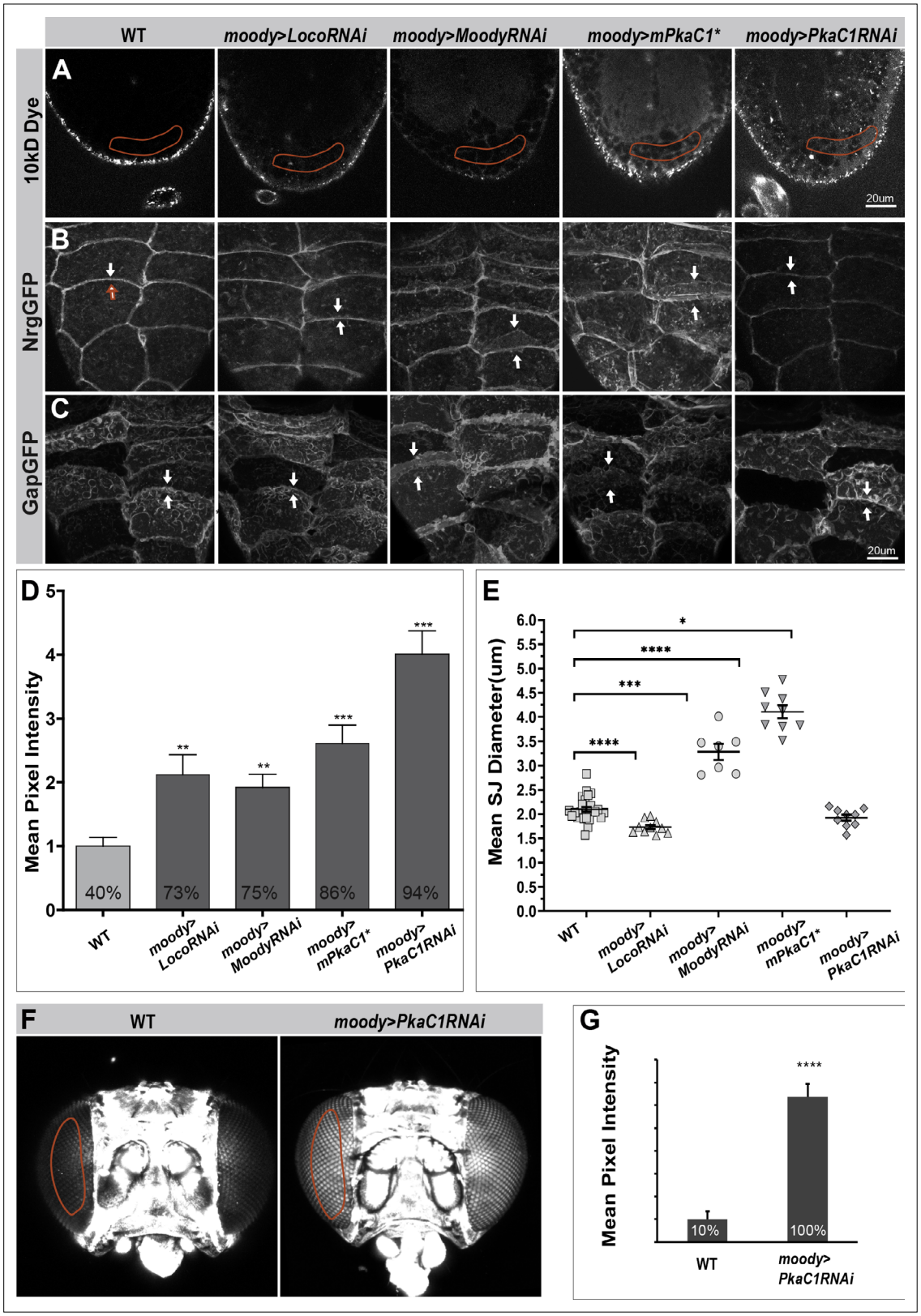

Figure 2. Moody/protein kinase A (PKA) signaling is required for blood–brain barrier (BBB) growth in the larva and for BBB maintenance in the adult. (**A**) Single confocal sections of dye-injected third instar larval nerve cords under different Moody/PKA activity levels. (**B, C**) Morphology of subperineural glia (SPG) septate junction (SJ) belts and membrane overlap at different Moody/PKA activity levels, as visualized by SJ markers NrgGFP (**B**), and the membrane marker GapGFP (**C**). (**D**) Quantification of the dye penetration assay. Columns represent intensity of dye penetration as measured by mean

Figure 2 continued on next page

Figure 2 continued

pixel intensity (see Experimental procedures), ± SEM, n = 44–88. The percentage of larva showing dye penetration is indicated at the bottom of each column. (**E**) Quantification of the diameter of SJ belts under different GPCR/PKA activity levels, using the SJ marker NrgGFP.± SEM, n = 7–28. (**F**) Dye penetration in adult flies as shown in z-projections of dye-injected adult heads. (**G**) Quantification of dye penetration in adult eye. Columns represent intensity of dye penetration as measured by mean pixel intensity in each adult eye (see Experimental procedures), ± SEM, n = 30 and 18. Asterisks in (**D**), (**E**), and (**G**) indicate significance levels of comparisons based on Welch's ANOVA with Dunnett's T3 multiple comparisons test (**D**) and (**E**) or the two-tailed unpaired t-test (**G**), n.s., $p>0.05$; *$p<0.05$; **$p<0.01$, ***$p<0.001$, ****$p<0.0001$.

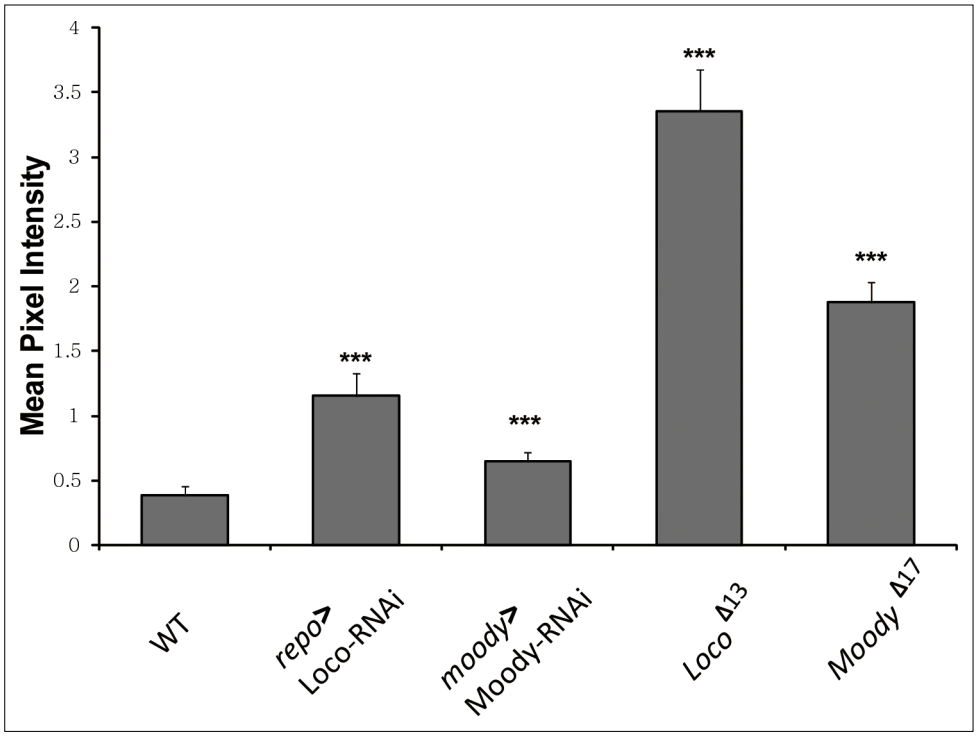

Figure 2—figure supplement 1. Dye penetration defects for RNAi vs. genomic mutants in the embryo. Graph shows quantification of penetration of fluorescent dye into the CNS in WT, loco, and moody null alleles, as well as loco or moody-RNAi expressed under repo- or moody-Gal4; 22 hr embryos. While moody-RNAi expressed using moody-Gal4 results in measurable dye penetration, the defect is much milder than in the mutant. Asterisks indicate statistical significance levels as assessed by one-way ANOVA with Dunnett's multiple comparisons test, n.s., $p>0.05$; *$p<0.05$; **$p<0.01$; ***$p<0.001$.

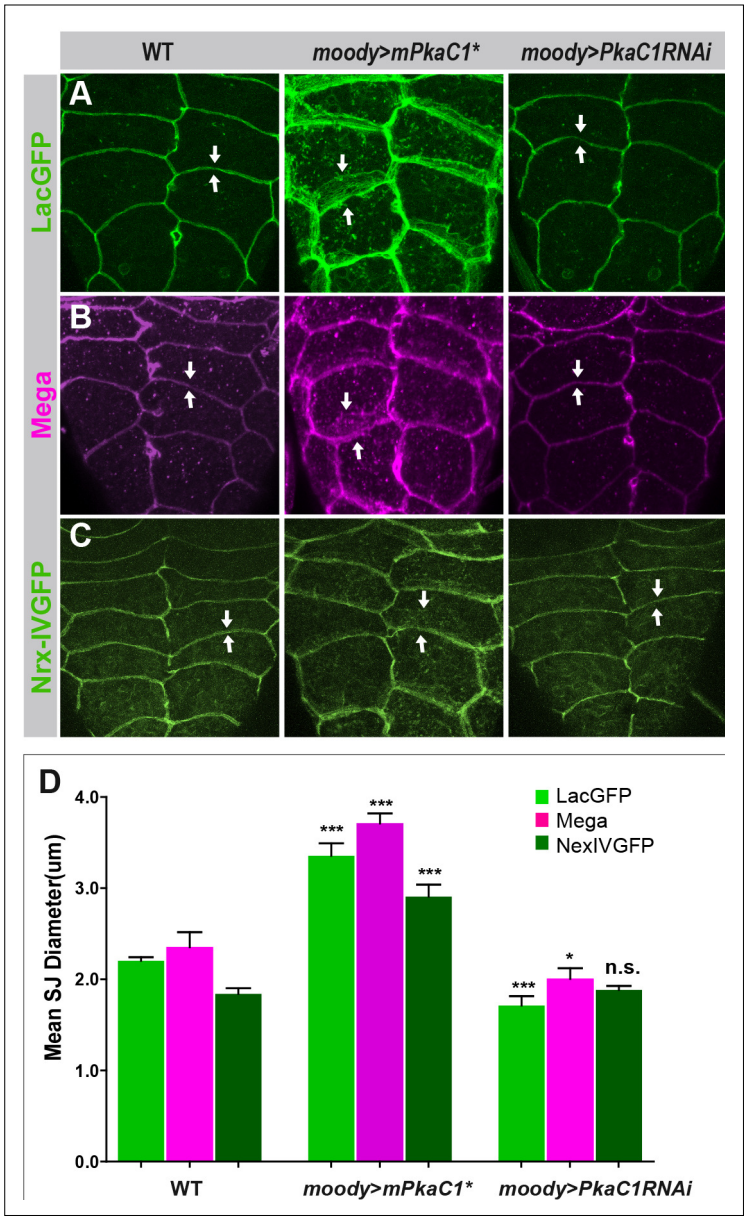

Figure 2—figure supplement 2. Morphology of subperineural glia (SPG) septate junction (SJ) belts at different protein kinase A (PKA) activity levels, as visualized by SJ markers LacGFP (**A**), Mega (**B**), and Nrx-IVGFP (**C**). (**D**) Quantification of the diameter of SJ belts under different PKA activity levels, using different SJ markers. All groups in PKA overactivity and one group of LacGFP labeled SJ belt in PKA underactivity are significantly different from WT, as assessed by Welch's ANOVA with Dunnett's T3 multiple comparisons test, n.s., $p>0.05$; *$p<0.05$; **$p<0.01$, ***$p<0.001$.

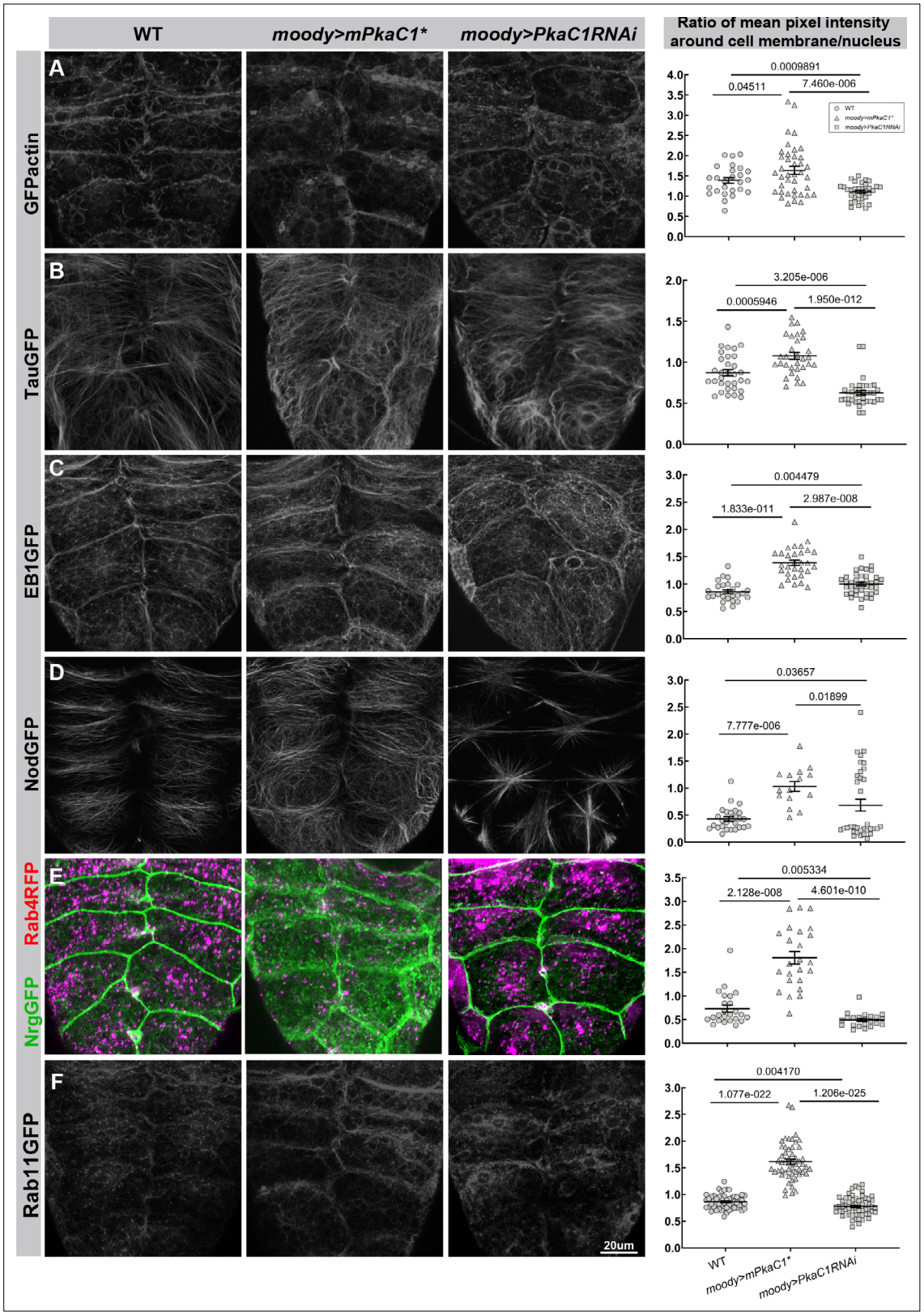

Figure 3. Protein kinase A (PKA) regulates the cytoskeleton and vesicle distribution in subperineural glia (SPG). Under different PKA activity levels, the actin cytoskeleton is visualized by GFPactin (**A**), the microtubule cytoskeleton by the general MT marker TauGFP (**B**), the plus-end marker EB1GFP (**C**), and the minus-end marker NodGFP (**D**), the cellular distribution of vesicles by the early endosome markers Rab4RFP (**E**) and Rab11GFP (**F**) with the septate junction (SJ) marker NrgGFP labeling the cell periphery of the SPG (**E**). (**G**) Quantification of the distribution of all markers around membrane

Figure 3 continued on next page

Figure 3 continued

area and the nucleus area under different PKA activity levels, including GFPactin, TauGFP, EB1GFP, NodGFP, Rab4RFP, and Rab11GFP. Columns represent the ratio of mean pixel intensity around cell membrane/nucleus in random SPG cells, ± SEM, n = 22–54. Asterisks indicate significance levels of comparisons based on Brown–Forsythe and Welch's ANOVA with multiple comparisons test, p value is label in each comparison group. A strong cortical actin rim around cell periphery is visible in WT (**A**). Compared with WT, the cortical actin rim is wider and stronger upon increased PKA activity and becomes weaker and less regular with reduced PKA activity. In WT (**B**–**D**), TauGFP-labeled microtubule fibers extend from MTOC to cell periphery throughout the cytoplasm (**B**); EB1GFP is enriched at the cell cortex but visible throughout the cytoplasm (**C**); NodGFP is enriched on fibers around the nucleus, but not around the cell cortex (**D**). Upon increased PKA activity, EB1GFP shows broader and more diffuse localization at the cell cortex, TauGFP and NodGFP become enriched at the cell periphery and show a web-like structure throughout the cytoplasm. Upon reduced PKA activity, TauGFP reveals disorganized and wavy microtubule organization; EB1 localization at the cell cortex is reduced; NodGFP accumulates around the MTOC in a striking star-shaped fashion. Rab4RFP- and Rab11GFP-labeled endosomes are differentially enriched in the cell periphery under PKA overactivity and surrounding the nucleus under reduced PKA activity when compared to its broader pan-cytoplasmic distribution in WT (**E, F**).

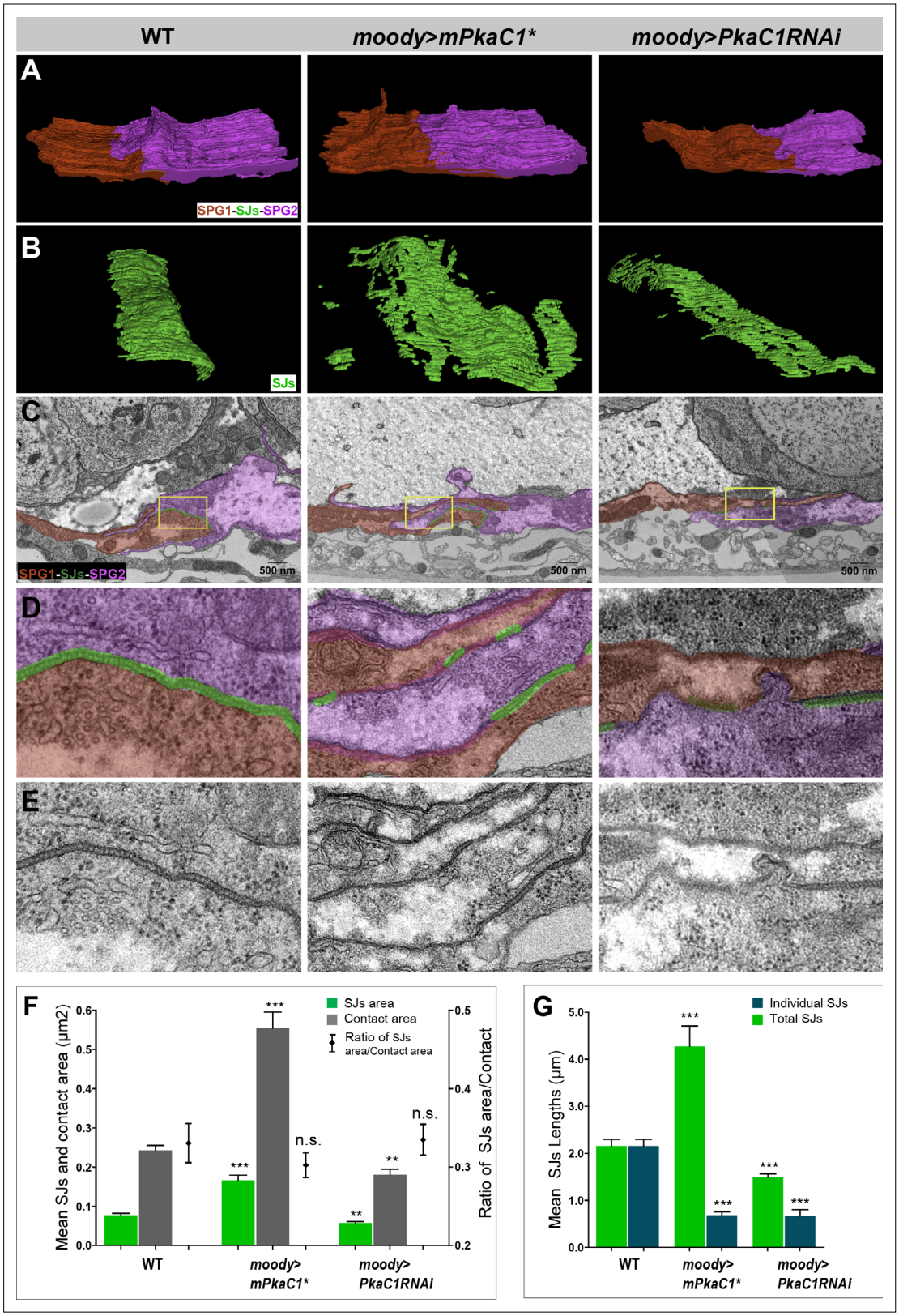

Figure 4. The continuity of the septate junction (SJ) belt is essential for blood–brain barrier (BBB) function as revealed by serial section transmission electron microscopy (ssTEM). (**A–E**) SJ ultrastructure at the interface of neighboring subperineural glia (SPG) in third instar larvae under different protein kinase A (PKA) activity levels. SPG1, its neighbor SPG2, and their shared SJs are colored or shaded in red, magenta, and green, respectively. (**A, B**) A 3D model of SJ ultrastructure generated by ssTEM. (**C**) Representative sections of SJs. (**D, E**) High-magnification views of boxed regions in (**C**) with and

Figure 4 continued on next page

Figure 4 continued

without shading. In WT, the area of contacting SPG is compact and well defined, and a dense SJ belt is formed between neighboring SPG. Under PKA overactivity (moody>mPkaC1*), neighboring SPG show much deeper interdigitations, and the SJs belt are discontinuous and appear patchy. Under PKA underactivity (*moody>PkaC1* RNAi), the cell contact and SJ area are reduced, and the SJ belt becomes patchy too. (**F**) Quantification of SJ surface area (green column) and the contact area (grey column), and the ratio between these two area (black point) under different PKA activity levels, ± SEM, n = 15–21. (**G**) Quantification of the mean length of individual SJ segments (green) and the mean total length of SJs (blue) under different PKA activity levels, measured in random nerve cord sections, ± SEM, n = 9–92. Asterisks in (**F, G**) indicate significance levels of comparisons based on Welch's ANOVA with Dunnett's T3 multiple comparisons test, n.s., $p>0.05$; *$p<0.05$; **$p<0.01$, ***$p<0.001$. Compared to WT, the mean total length of SJs significantly increases (4.28 ± 0.43 μm vs. 2.16 ± 0.14 μm, $p=0.000523$, about twofold) and the mean length of individual SJ segments significantly decreases (0.69 ± 0.08 μm vs. 2.16 ± 0.14 μm, $p<0.0001$, about 0.3-fold) under PKA overactivity; both the mean total length of SJs (1.49 ± 0.08 μm vs. 2.16 ± 0.14 μm, $p=0.000878$, about 0.69-fold) and the mean length of individual SJ segments decrease (0.67 ± 0.14 μm vs. 2.16 ± 0.14 μm, $p<0.0001$, about 0.31-fold), respectively, upon reduced PKA activity.

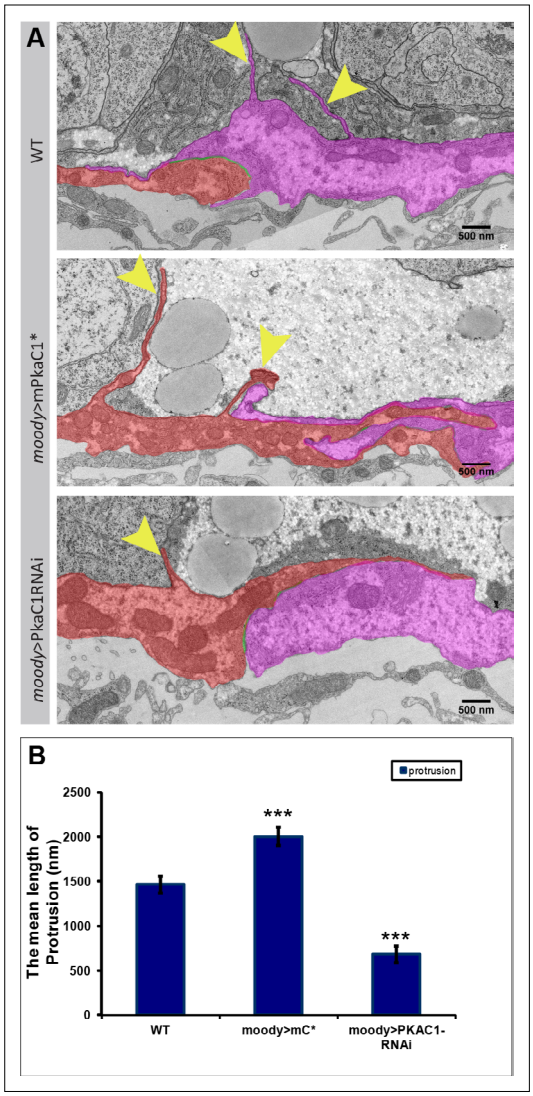

Figure 4—figure supplement 1. Morphology of apical membrane protrusions of subperineural glia (SPG) at different protein kinase A (PKA) activity levels, as revealed by serial section transmission electron microscopy (ssTEM). (**A**) Representative sections of the apical membrane protrusion of SPG ultrastructure under different PKA levels, marked by yellow arrows. SPG1, its neighbor SPG2, and their shared SJs are colored in red, magenta, and green, respectively. (**B**) Quantification of the mean length of individual apical protrusion under different PKA activity levels, measured in random nerve cord sections, ± SEM, n = 14–35. Compared to WT, the mean length of apical membrane protrusion of SPG is significantly longer under PKA overactivity and significantly shorter under PKA underactivity. Statistical significance of comparisons was assessed using Welch's ANOVA with Dunnett's T3 multiple comparisons test, n.s., $p>0.05$; *$p<0.05$; **$p<0.01$, ***$p<0.001$.

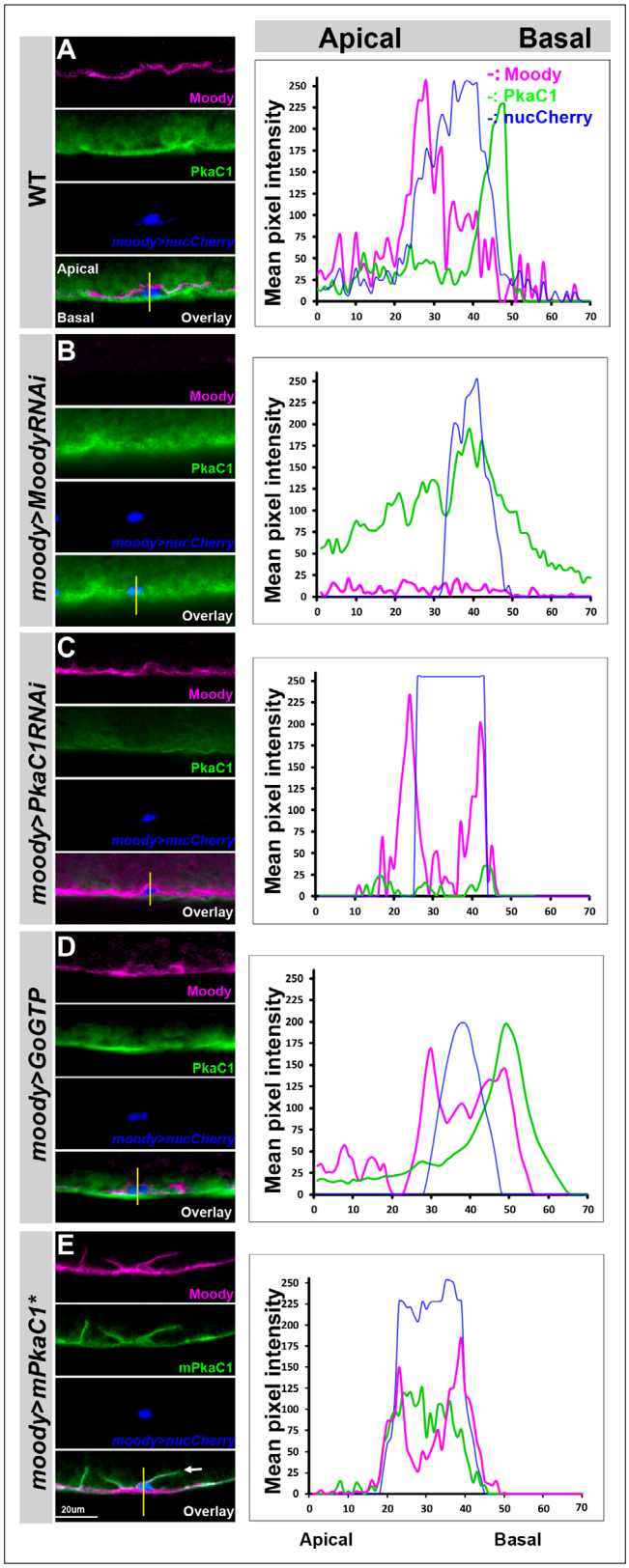

Figure 5. The Moody/protein kinase A (PKA) signaling pathway is polarized in subperineural glia (SPG). The subcellular localization of the PKA catalytic subunit PkaC1 and Moody in SPG of third instar larvae in WT (**A**), Moody knockdown (*moody>MoodyRNAi*) (**B**), PkaC1 knockdown (*moody*>Pka-C1-RNAi), GPCR gain of function (*moody*>Go GTP), and PKA overexpression (*moody*>mPka-C1*). Antibody labeling of Moody (magenta), of

Figure 5 continued on next page

Figure 5 continued

Drosophila PkaC1 or mouse PkaC1 (green), and of SPG nuclei (*moody>nucCherry*; blue). (**A–E**) Lateral views of the CNS/hemolymph border, with CNS facing top. On the right column, line scans of fluorescence intensities for each channel along the apical–basal axis at the positions indicated. In WT (**A**), Moody localizes to the apical side and PkaC1 is enriched at the basal side of SPG. Under loss of Moody signaling (*moody>MoodyRNAi*) (**B**), PKA spreads throughout the cell and loses its basal localization. Moody loses its apical localization under reduced (**C**) or increased PKA activity (**E**). Under GPCR gain of function (**D**), Pka-C1 is basally polarized, while Moody lost its asymmetric localization in SPG.

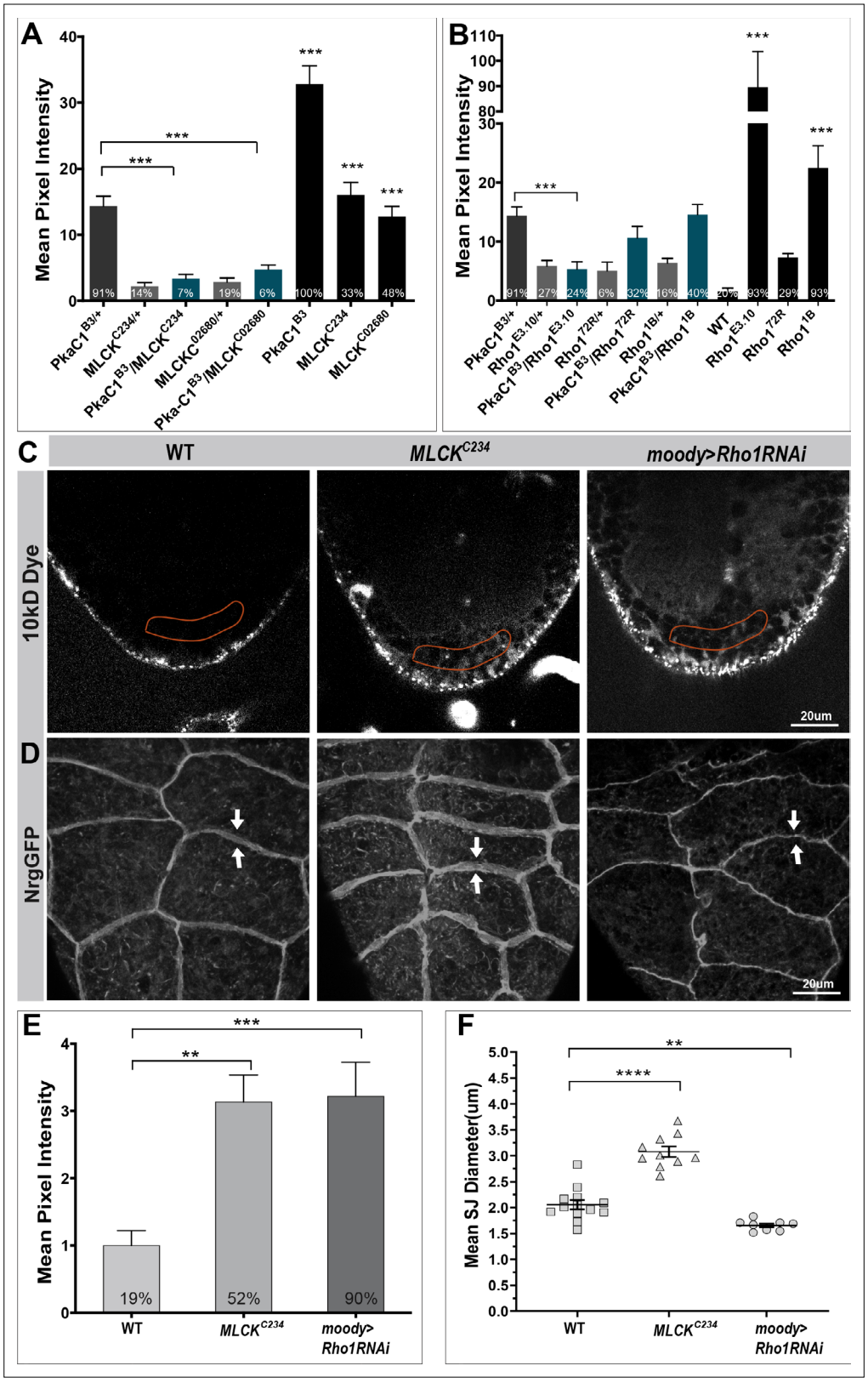

Figure 6. Myosin light chain kinase (MLCK) and Rho1 function as protein kinase A (PKA) targets in subperineural glia (SPG). (**A**) Quantification of dye penetration effects in the embryo of *MLCK* and *Rho1*. (**B**) Dominant genetic interactions between *PkaC1*^{B3} and *MLCK* and *Rho1* mutant heterozygotes as quantified by dye penetration in the embryo. In (**A, B**), columns represent the strength of dye penetration into the nerve cord as measured by the

Figure 6 continued on next page

Figure 6 continued

mean pixel intensity, ± SEM, n = 14–98. (**C, D**) Blood–brain barrier (BBB) phenotype of *MLCK* zygotic mutant and SPG-specific Rho1 knockdown (*moody>Rho1* RNAi) animals in single confocal sections of dye injected third instar larvae (**C**), and septate junction (SJ) morphology using the NrgGFP marker (**D**), with width of SJ belt highlighted by arrows. (**E**) Quantification of the dye penetration assay from (**C**). Columns represent intensity of dye penetration as measured by mean pixel intensity and normalized to WT mean (see *Materials and methods*, ± SEM, n = 13–19). (**F**) Quantification of the mean diameter of SJ belts from (**D**), ± SEM, n = 8–13. In (**A**), (**B**), and (**E**), the percentage of animals showing dye penetration is indicated at the bottom of each column. Asterisks in (**A**), (**B**), (**E**), and (**F**) indicate significance levels of comparisons against either WT in (**E**) and (**F**) or $PkaC1^{B3}$ group in (**A**) and (**B**) based on Brown–Forsythe and Welch's ANOVA with multiple comparisons test, n.s., $p>0.05$; *$p<0.05$; **$p<0.01$, ***$p<0.001$.

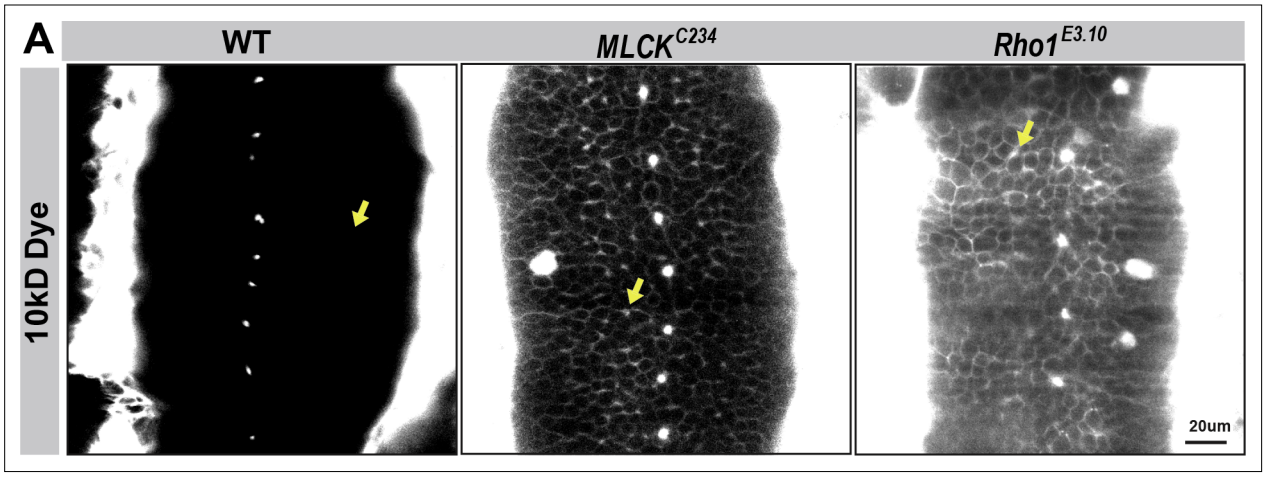

Figure 6—figure supplement 1. Myosin light chain kinase (MLCK) and Rho1 are required for blood–brain barrier (BBB) integrity in embryos. Single confocal section of dye-injected MLCKC234 zygotic mutant (*MLCK*^{C234}), and Rho1 zygotic null mutant (*Rho1*$^{E3.10}$) embryos, with dye penetrating into the nerve cord (yellow arrow) (**A**).

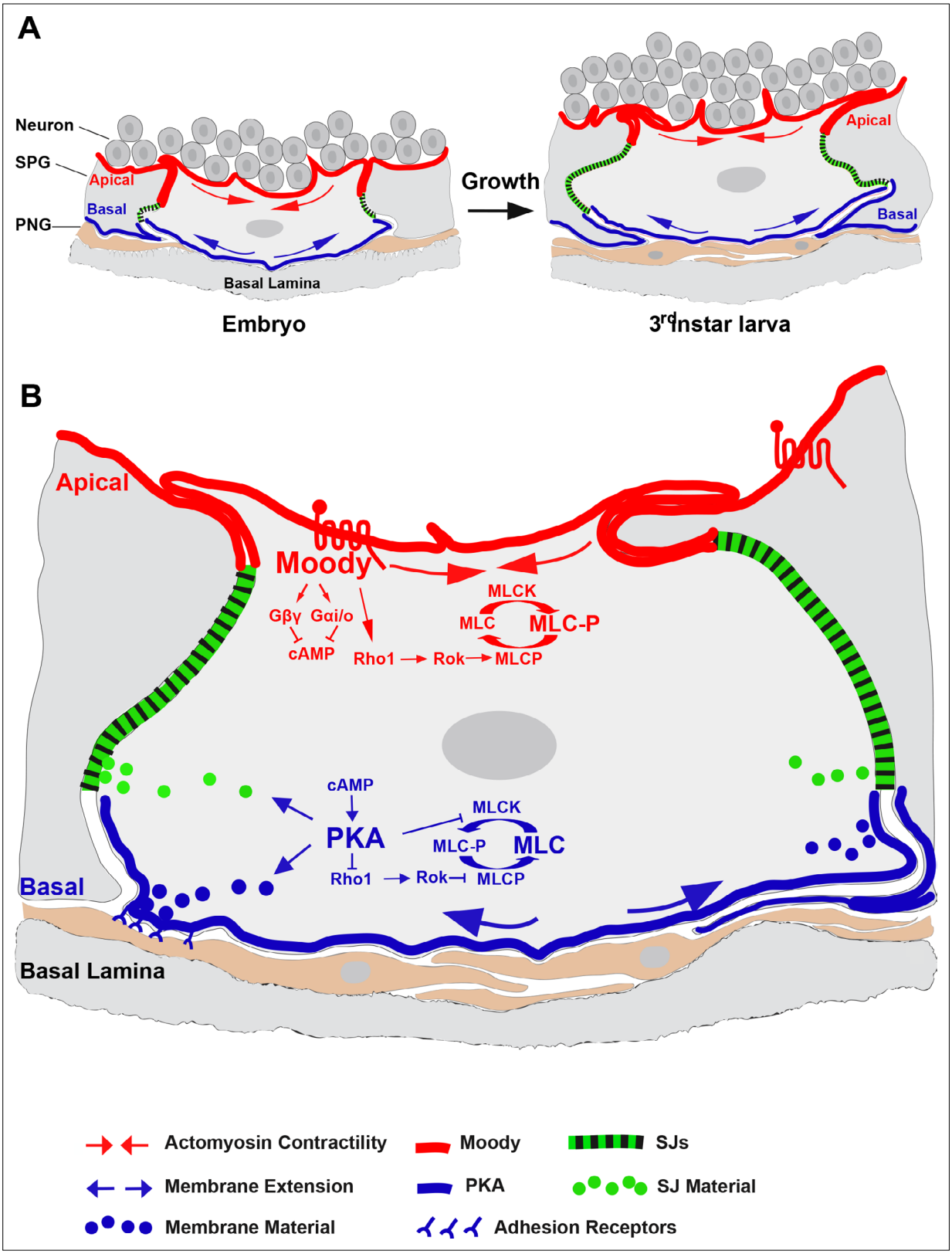

Figure 7. Model of Moody/protein kinase A (PKA) signaling in the glial blood–brain barrier (BBB). Schematic depicting polarized Moody/PKA signaling along the apical–basal axis and its cellular function in controlling subperineural glia (SPG) continued cell growth (**A**) and BBB integrity (**B**) by differentially regulating actomyosin contractility and septate junction (SJ) organization spatiotemporally. For detailed description, see Discussion.